

## Supporting Information

### **Modulating Crystallinity and Mixed Ionic-Electronic Conduction Properties by Terminal Side Chain Engineering of N-Type Small Molecules**

Xiuyuan Zhu<sup>‡</sup>, Junxin Chen<sup>‡</sup>, Riping Liu, Chaoyue Chen, Juntao Tan, Chong Ran,  
Yiming Wang, Runxia Wang, Zhengke Li, Wan Yue\*

State Key Laboratory of Optoelectronic Materials and Technologies, Key Laboratory for Polymeric  
Composite and Functional Materials of Ministry of Education, Guangzhou Key Laboratory of  
Flexible Electronic Materials and Wearable Devices, School of Materials Science and Engineering,  
Sun Yat-sen University, Guangzhou 510275, (P. R. China). E-mail: yuew5@mail.sysu.edu.cn.

## **Table of Contents**

- 1. Experimental Section**
- 2. Material Synthesis and Characterization**
- 3. TGA of Compounds**
- 4. CV of Compounds**
- 5. Detailed Data of GIWAXS Tests**
- 6. AFM of compounds**
- 7. Organic Electrochemical Transistors Characterization**
- 8. Organic Electrochemical Neuronal Synapse Characterization**
- 9. References**

## 1. Experimental Section

**Materials.** All raw materials were purchased from commercial suppliers and used as received unless otherwise specified. 1,5-naphthalenediamine (CAS: 2243-62-1) and tetraethylene glycol monomethyl ether (CAS: 23783-42-8) were purchased from Bide medical (Shanghai) Co., methyl bromoacetate (CAS: 96-32-2) was purchased from Macklin medical Co., n-propylamine (CAS: 107-10-8), n-butylamine (CAS: 109-73-9), n-amylamine (CAS: 110-58-7) and carbon disulfide (CAS: 75-15-0) were purchased from Aladdin medical Co. The spectroscopic grade solvents for spectroscopic studies were purchased from Sigma Aldrich and used as received. The intermediates and target compounds were purified by column chromatography on silica gel (General-Regent, 200–300 mesh).

**Material Structures and Optoelectronic Properties.**  $^1\text{H}$  and  $^{13}\text{C}$  Nuclear Magnetic Resonance spectra were recorded in chloroform-d with a 600 MHz Bruker Advance III HD spectrometer. Mass spectra were recorded on a Bruker Solarix XR mass spectrometer (with Electrospray ionization and Atmospheric pressure chemical ionization mode). Thermogravimetric Analysis was carried out at a rate of  $10\text{ }^\circ\text{C min}^{-1}$  under nitrogen atmosphere with a Thermogravimetric analyzer from Nicolet 6700. The thin films of the small molecular semiconductors reported in this work were prepared by spin-coating on substrates at the rate of 500 rpm for 5 s and 1000 rpm for 30 s from their hexafluoroisopropanol solutions ( $10\text{ mg ml}^{-1}$ ) under ambient conditions. Ultraviolet Visible Absorption Spectroscopies were captured by an Agilent Technologies Cary Series UV-Vis-NIR spectrophotometer. Cyclic Voltammetry measurements in solution state were carried out *via* a three-electrode system holding palladium carbon as working electrode, platinum wire as counter electrode and Ag/AgCl as reference electrode (internally calibrated against ferrocene) with a standard commercial electrochemical analyzer (Shanghai Chenhua Instrument co. LTD., CHI600E). while those in solid state used ITO glass slides spin-coated with  $0.5\text{ cm}^2$  of small molecule thin films as working electrode. In solution state and solid state, 0.1 M tetrabutylammonium hexafluorophosphate ( $\text{TBAPF}_6$ ) in deoxygenated chloroform and

0.1 M NaCl aqueous solution were used as the electrolyte respectively. Spectro-Electrochemical measurements were performed using the UV-Vis-NIR spectrophotometer coupled with the electrochemical analyzer potentiostat in a three-electrode setup. On ITO-coated glass slides were deposited the small molecular semiconductors, and then the glass slides were inserted in a quartz cuvette equipped with a custom-made Teflon lid, using platinum wire as counter electrode and Ag/AgCl electrode as reference electrode, which were both immersed in 0.1 M NaCl aqueous solution. The background measurement was conducted with a clean bare ITO-coated glass slide in 0.1 M NaCl aqueous solution. Before measuring the spectrum, the indicated voltage was applied for ~30 s until the current was stabilized.

**Preparation of ion-gel electrolyte.** The 20 wt% gelatin (4 g) was dissolved in deionized water (16 mL) and the blend was heated at 60 °C until it turned into a clear solution which was cast into a mold and cooled at 4 °C for 1 h to obtain the hydrogel. After immersing the as-made hydrogels in 0.2 M NaCl solution with 60% v/v glycerol for 3 h at room temperature, the ion-gel electrolyte was prepared to be geared up.

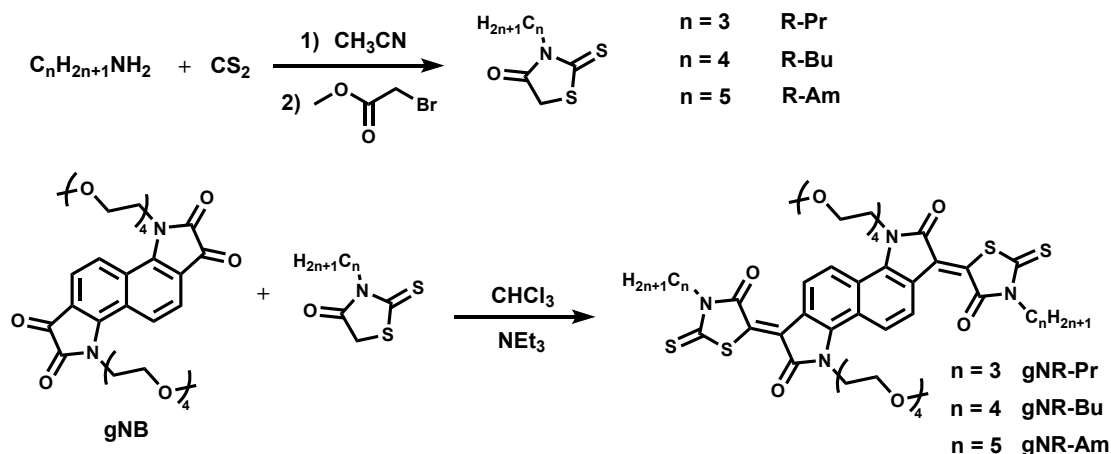
**Device Fabrication and Characterization.** The OECT and OENS fabrications both involved the deposition of gold as drain-source electrodes and small molecule semiconductors as the active layers, while OECT utilized patterned interdigitated electrodes and OENS required extra golden gate electrode. The substrate was cleaned by piranha solution and then dried by nitrogen gun. Gold was thermally evaporated onto the glass substrates and patterned with a standard photolithographic/lift-off process. The active channel layer was spin-coated at the rate of 500 rpm for 5 s and 1000 rpm for 30 s from a 10 mg ml<sup>-1</sup> hexafluoroisopropanol solution. The channel lengths and widths of the devices were 20 μm and 39000 μm, respectively. The OECT devices worked in aqueous electrolyte gated mode with 0.1 M NaCl aqueous solution as electrolyte and platinum wire as gate electrode, while the OENS devices with side gate plana structures worked in ion-gel gated mode with dissolved small molecule semiconductor spin-coated onto the channel layer and the aforementioned ion-gel

electrolyte covered on the whole surface. Device characterization was performed in air at room temperature using two semiconductor parametric analyzers (Keithley B1500A for OECT and Keithley 2612B for OENS) and an electrical probe station.

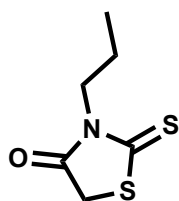
**Electrochemical Impedance Spectroscopy Measurements.** EIS measurements were carried out in 0.1 M NaCl aqueous solution *via* a three-electrode system holding gold coated glass slides as working electrode, platinum wire as counter electrode and Ag/AgCl as reference electrode with an electrochemical analyzer (Shanghai Chenhua Instrument co. LTD., CHI520E). The working electrode was spin-coated with 0.2 cm<sup>2</sup> of small molecule thin films. EIS measurements were performed at a DC offset potential of 0.55 V and a sinusoidal AC amplitude of 10 mV with the frequency ranging from 10 kHz to 0.1 Hz. The capacitance was determined using the equation  $C^* = 1/(2\pi f \text{Img}(Z))$ , where  $f$  is the frequency and  $Z$  is the complex impedance and calculated by EIS spectrum fitting based on the Randles circuit  $R_s (R_p||C)$  by the ZSimDemo software.

**Atomic Force Microscope Measurements and Grazing-Incidence Wide Angle X-ray Scattering Characterization.** The small molecule thin films were spin-coated on n<sup>+</sup> doped silicon wafer substrates from their 10 mg ml<sup>-1</sup> hexafluoroisopropanol solution at the rate of 500 rpm for 5 s and 1000 rpm for 30 s under ambient conditions. AFM measurements were carried out by Bruker dimension icon Atomic Force Microscope in tapping mode with a silicon tip. were used to record the scattering patterns. The 2D GIWAXS patterns were collected with the film resistivity of 0.001–30 Ohm cm<sup>-1</sup>, the incidence angle of 0.18° and the photon energy of 8 keV.

## 2. Material Synthesis and Characterization



**Scheme S1.** Synthetic route of alkyl substituted rhodanine and corresponding **gNR** derivatives. **gNB** were synthesized according to the literature. [1] **R-Bu** and **gNR-Bu** were already reported in our previous work. [2]



### R-Pr

In a 25 mL round-bottomed flask was added 1-propylamine (1 mL, 12.2 mmol), acetonitrile (10 mL, solvent), and carbon disulfide (1.9 mL, 31.5 mmol). The mixture was stirred at room temperature until the raw materials disappeared determined by thin layer chromatography to give a yellow liquid. Then methyl bromoacetate (1 mL, 10.5 mmol) was added and the blend was heated at 80 °C overnight. The solvent was then evaporated under vacuum, and the residue was purified by column chromatography (silica gel, Ethyl Acetate: n-Hexane = 1:5). The final product was obtained as a yellow sticky liquid (908 mg, 5.2 mmol, yield = 50%).

$^1H$  NMR (600MHz, Chloroform-d, 300K),  $\delta$  (ppm): 3.97 (d,  $J = 15.6$  Hz, 4H), 1.70 (h,  $J = 7.5$  Hz, 2H), 0.96 (t,  $J = 7.4$  Hz, 3H).  $^{13}C$  NMR (150 MHz, Chloroform-d, 300K),  $\delta$  (ppm): 201.24, 173.88, 46.21, 35.29, 20.15, 11.15.

ESI-MS: Calculated for  $C_6H_9NOS_2$ : 175.01, found  $[M+H]^+$ : 176.02.

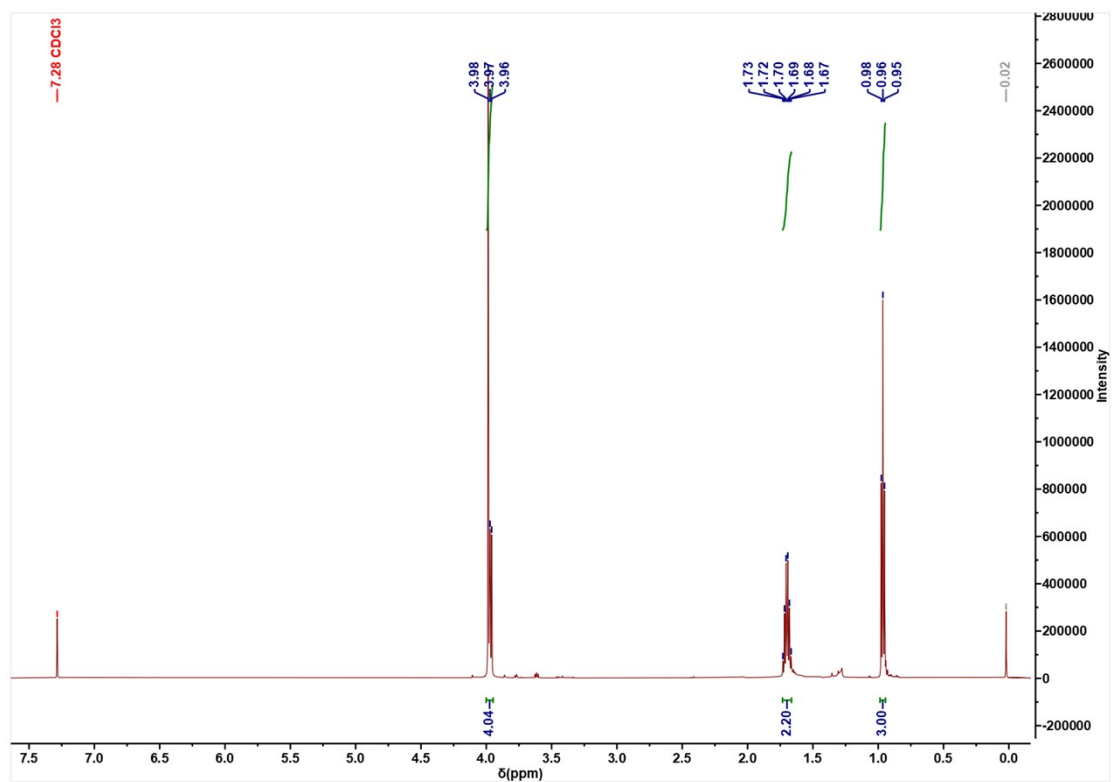


Figure S1.  $^1\text{H}$  NMR of R-Pr at 300K.

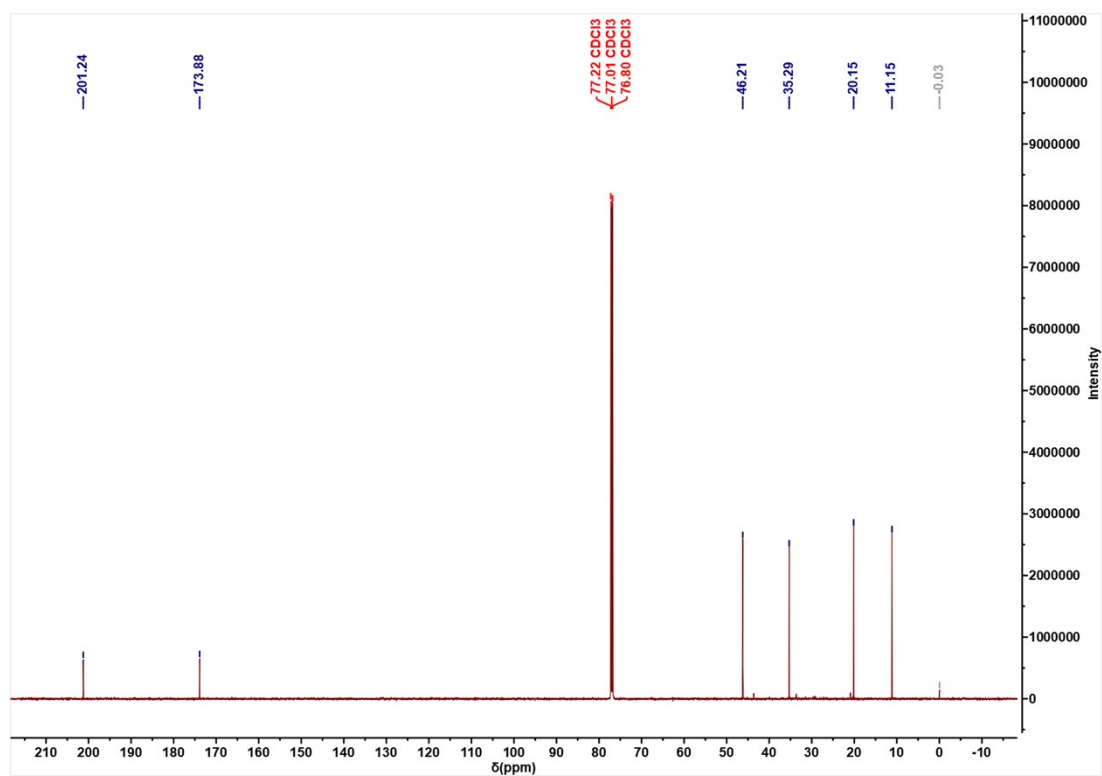
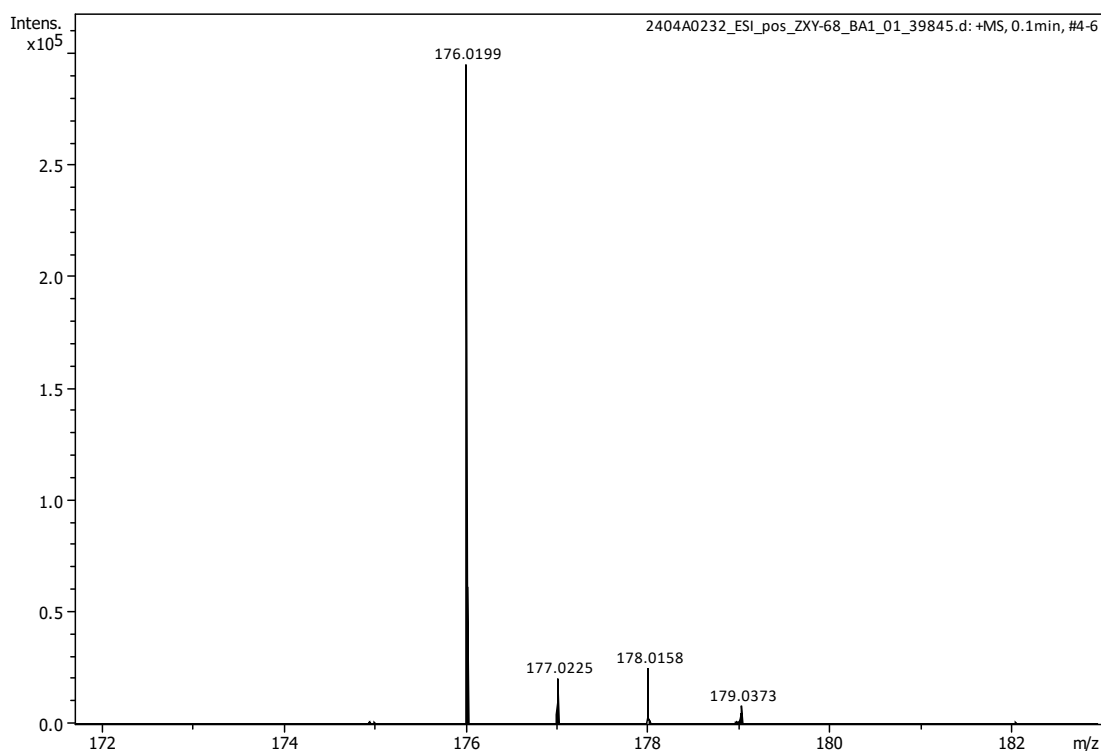
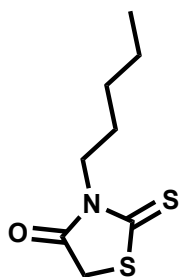


Figure S2.  $^{13}\text{C}$  NMR of R-Pr at 300K.



**Figure S3.** ESI-MS of **R-Pr**.



### **R-Am**

**R-Am** was synthesized according to compound **R-Pr**. The final product was obtained as a yellow sticky liquid (yield: 44%).

$^1\text{H}$  NMR (600 MHz, Chloroform-d, 300K),  $\delta$  (ppm): 3.99 (d,  $J = 9.2$  Hz, 4H), 1.65 (t,  $J = 7.7$  Hz, 2H), 1.34 (dq,  $J = 13.8, 6.6, 5.9$  Hz, 4H), 0.91 (t,  $J = 7.0$  Hz, 3H).  $^{13}\text{C}$  NMR (150 MHz, Chloroform-d, 300K),  $\delta$  (ppm): 201.24, 173.88, 44.77, 35.35, 28.84, 26.39, 22.22, 13.90.

ESI-MS: Calculated for  $\text{C}_8\text{H}_{13}\text{NOS}_2$ : 203.04, found  $[\text{M}+\text{H}]^+$ : 204.05.

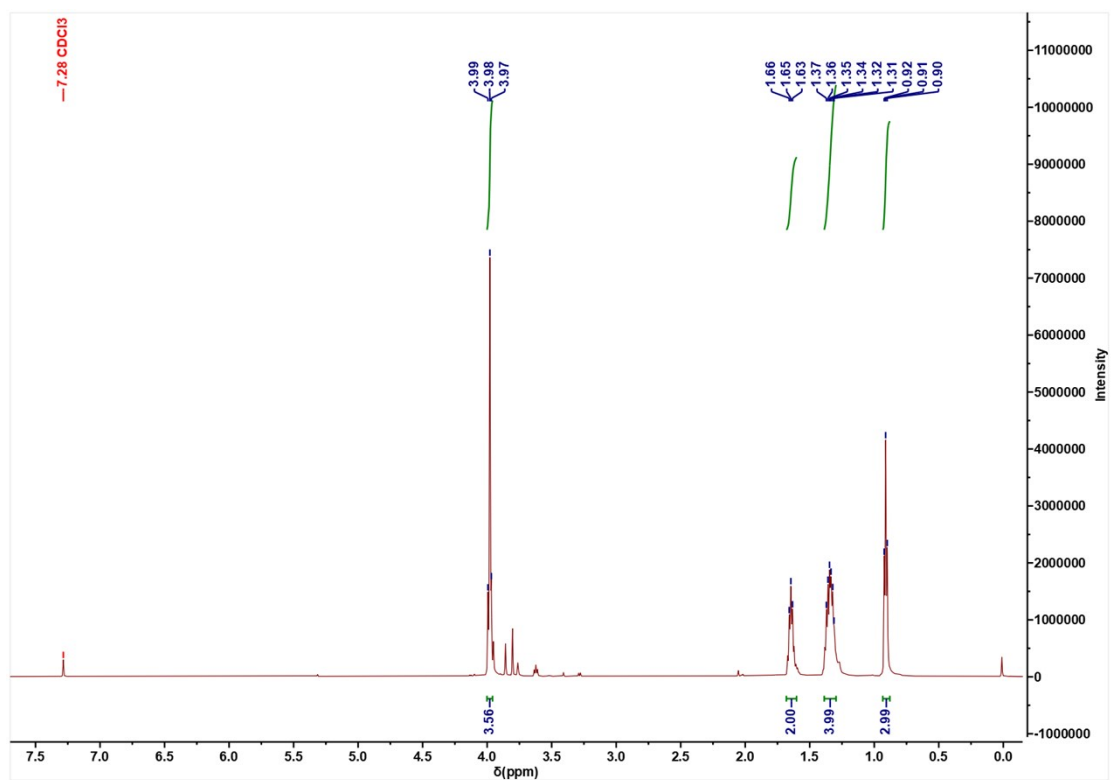


Figure S4.  $^1\text{H}$  NMR of R-Am at 300K.

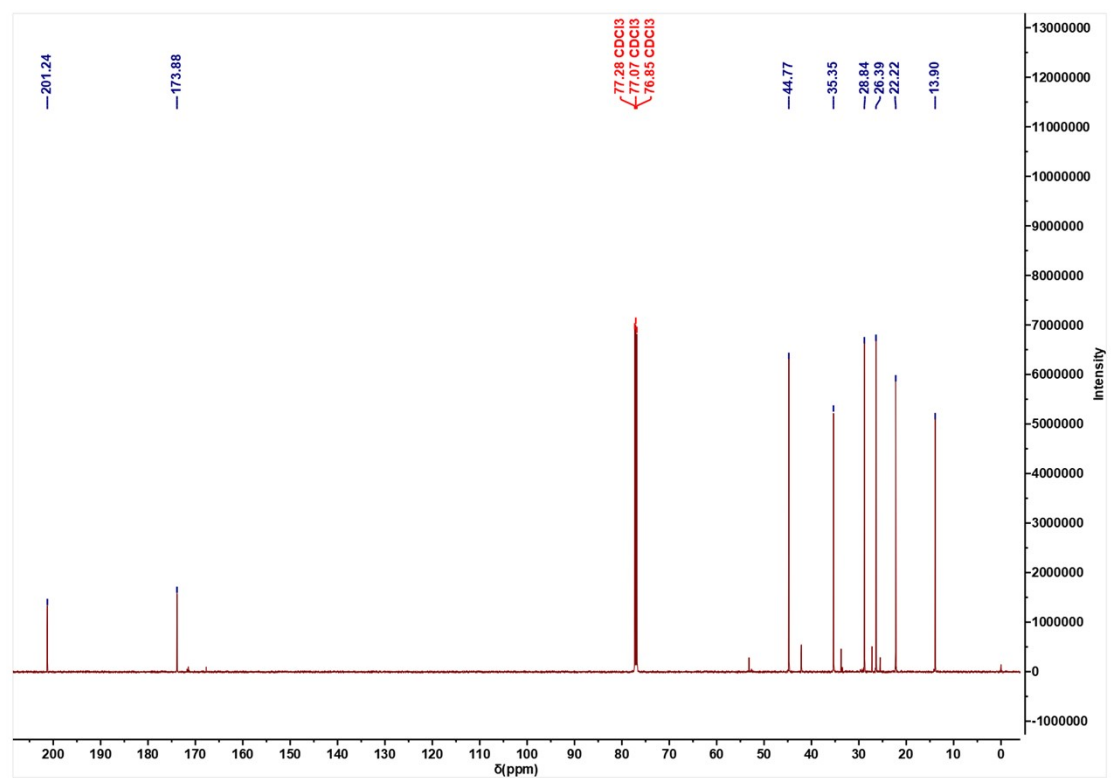
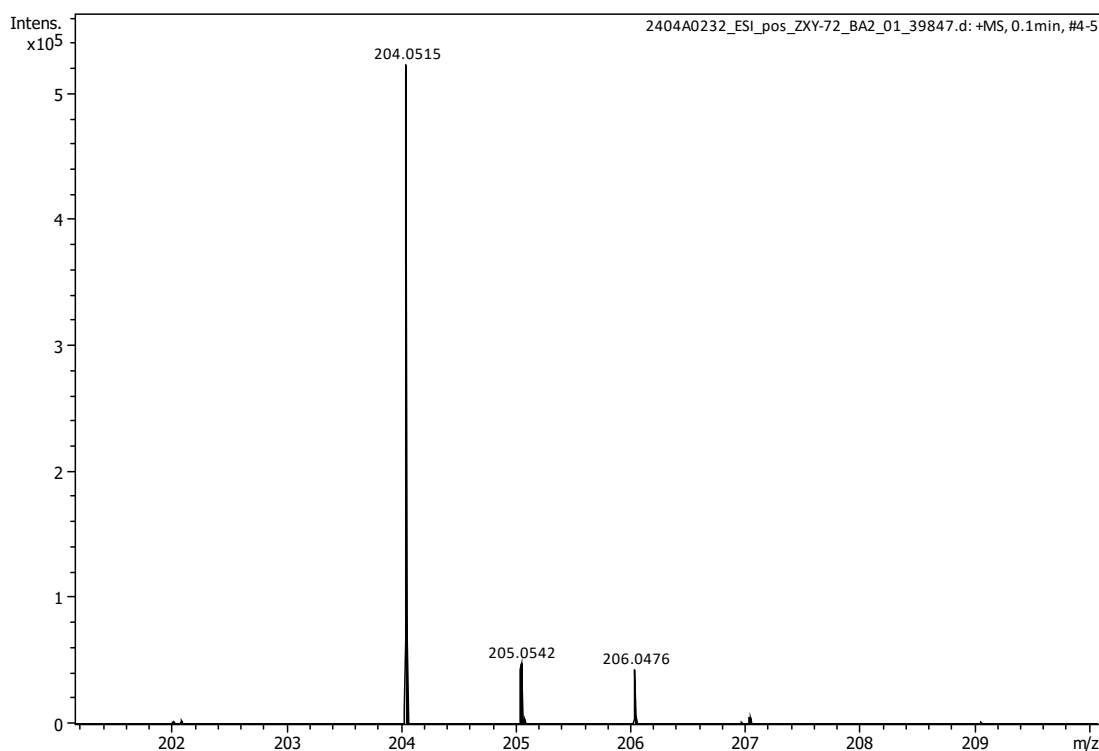
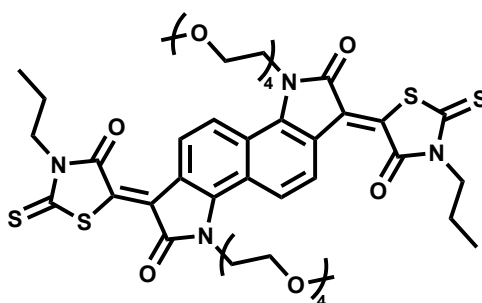


Figure S5.  $^{13}\text{C}$  NMR of R-Am at 300K.



**Figure S6.** ESI-MS of **R-Am**.



### **gNR-Pr**

In a 50mL flame-dried Schlent flask was added **gNB** (102 mg, 0.16 mmol), **R-Pr** (90 mg, 0.48 mmol), anhydrous chloroform (10 mL, solvent), and triethylamine (0.04 mL, catalyzer) under nitrogen atmosphere. The mixture was subsequently heated and stirred at 65 °C to reflux. The termination of the reaction was determined as the disappearance of raw materials by thin layer chromatography. Then the blend was purified by column chromatography (silica gel, Dichloromethane: Methanol = 50:1) to give a raw product which was further washed with methanol and filtered. The final product was obtained as a green sticky solid (80 mg, 0.08 mmol, yield = 50%).

<sup>1</sup>H NMR (600 MHz, Chloroform-d, 300K),  $\delta$  (ppm): 8.93 (d,  $J$  = 9.0 Hz, 2H), 7.94 (d,

$J = 9.2$  Hz, 2H), 4.54 (t,  $J = 6.2$  Hz, 4H), 4.13 (t,  $J = 7.7$  Hz, 4H), 3.93 (t,  $J = 6.2$  Hz, 4H), 3.71 (t,  $J = 4.6$  Hz, 4H), 3.63 (d,  $J = 9.3$  Hz, 16H), 3.54 (t,  $J = 4.7$  Hz, 4H), 3.37 (s, 6H), 1.80 (h,  $J = 7.6$  Hz, 4H), 1.05 (t,  $J = 7.4$  Hz, 6H).  $^{13}\text{C}$  NMR (150 MHz, Chloroform-d, 300K),  $\delta$  (ppm): 196.27, 168.91, 166.98, 143.09, 134.31, 123.71, 122.73, 122.44, 118.08, 117.59, 71.91, 70.75, 70.61, 70.54, 70.50, 68.73, 59.06, 46.05, 43.52, 29.34, 20.65, 11.37.

APCI-MS: Calculated for  $\text{C}_{44}\text{H}_{56}\text{N}_4\text{O}_{12}\text{S}_4$ : 960.28, found  $[\text{M}+\text{H}]^+$ : 961.29.

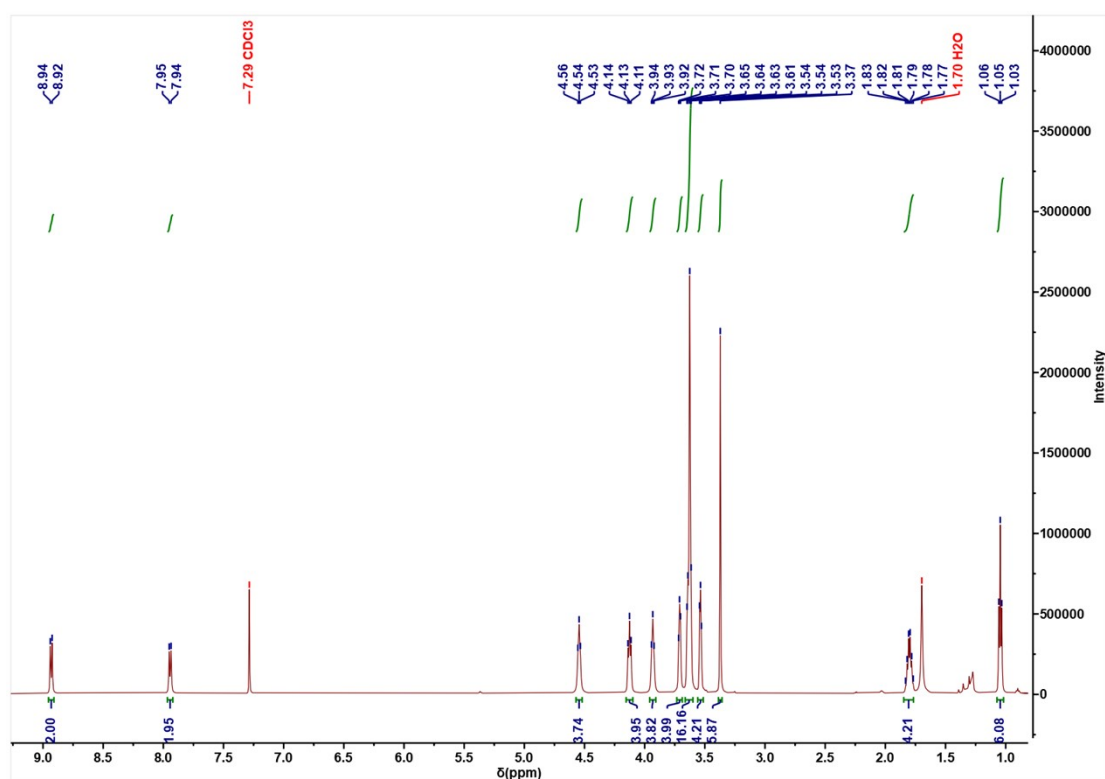


**Figure S7.**  $^1\text{H}$  NMR of **gNR-Pr** at 300K.

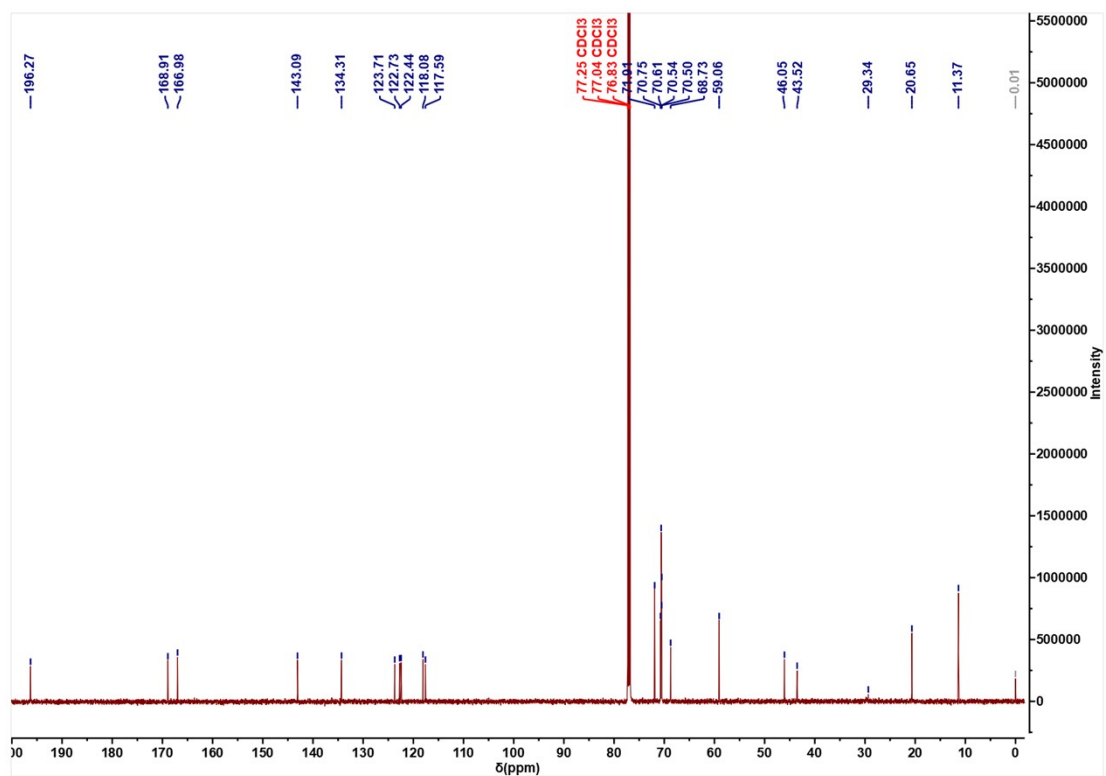


Figure S8.  $^{13}\text{C}$  NMR of gNR-Pr at 300K.

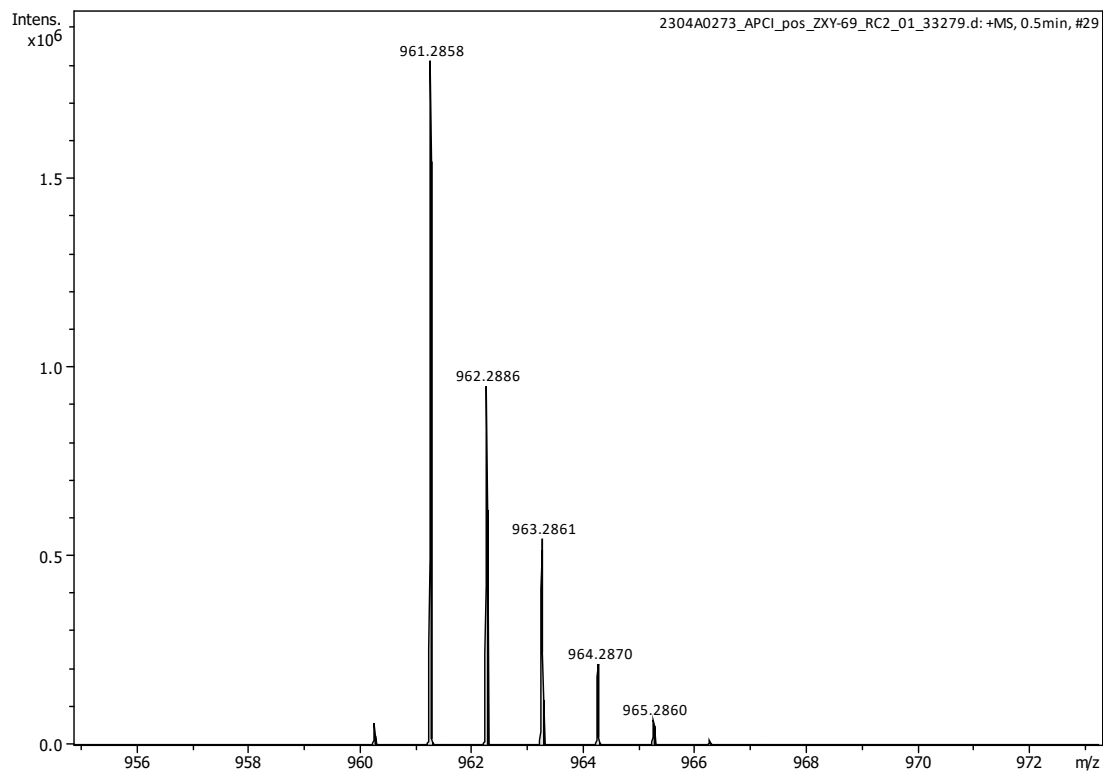
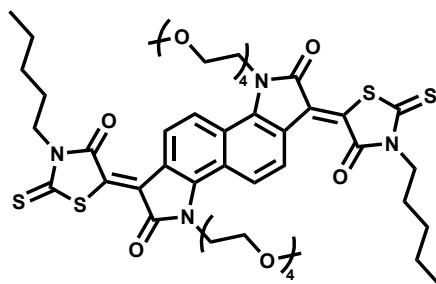


Figure S9. APCI-MS of gNR-Pr.



### gNR-Am

**gNR-Am** was synthesized according to compound **gNR-Pr**. The final product was obtained as green sticky solid (yield: 40%).

$^1\text{H}$  NMR (600 MHz, Chloroform- $d$ , 300K),  $\delta$  (ppm): 8.94 (d,  $J = 9.1$  Hz, 2H), 7.95 (d,  $J = 9.2$  Hz, 2H), 7.29 (s, 2H), 4.55 (t,  $J = 6.3$  Hz, 4H), 4.15 (t,  $J = 7.8$  Hz, 4H), 3.93 (t,  $J = 6.3$  Hz, 4H), 3.71 (dd,  $J = 5.9, 3.6$  Hz, 4H), 3.66 – 3.60 (m, 16H), 3.53 (dd,  $J = 5.8, 3.5$  Hz, 4H), 3.37 (s, 6H), 1.76 (q,  $J = 7.6$  Hz, 4H), 1.43 (dt,  $J = 7.9, 3.6$  Hz, 8H), 0.99 – 0.94 (m, 9H).  $^{13}\text{C}$  NMR (150 MHz, Chloroform- $d$ , 300K),  $\delta$  (ppm): 196.22, 168.92, 166.94, 143.09, 134.33, 123.74, 122.74, 122.45, 118.11, 117.59, 71.91, 70.74, 70.61, 70.54, 70.51, 68.72, 59.06, 44.60, 43.50, 28.98, 26.85, 22.32, 13.98.

APCI-MS: Calculated for  $\text{C}_{48}\text{H}_{64}\text{N}_4\text{O}_{12}\text{S}_4$ : 1016.34 found  $[\text{M}+\text{H}]^+$ : 961.29.

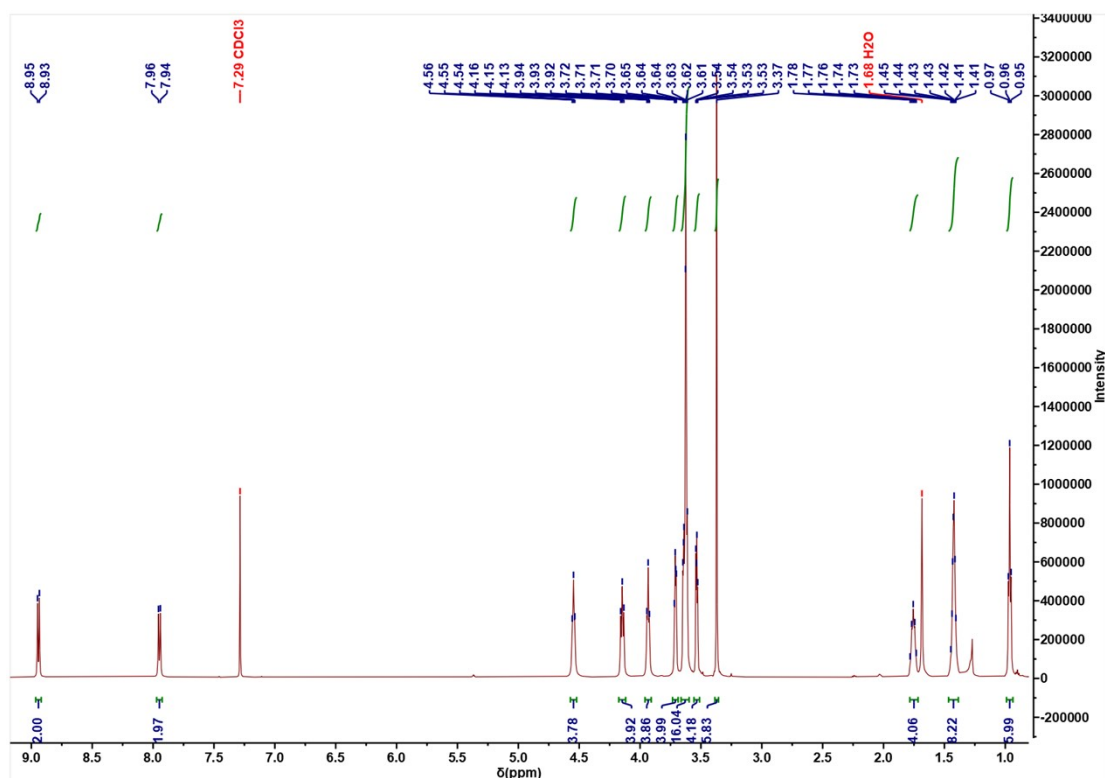


**Figure S10.**  $^1\text{H}$  NMR of **gNR-Am** at 300K.

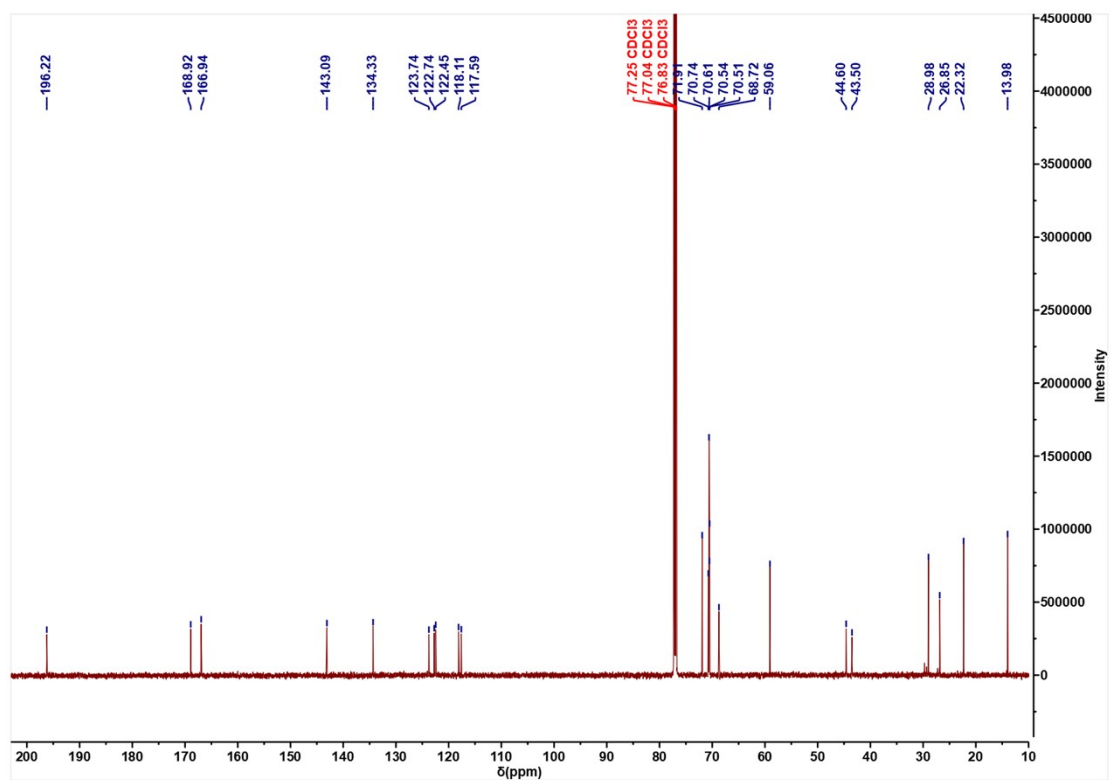


Figure S11.  $^{13}\text{C}$  NMR of gNR-Am at 300K.

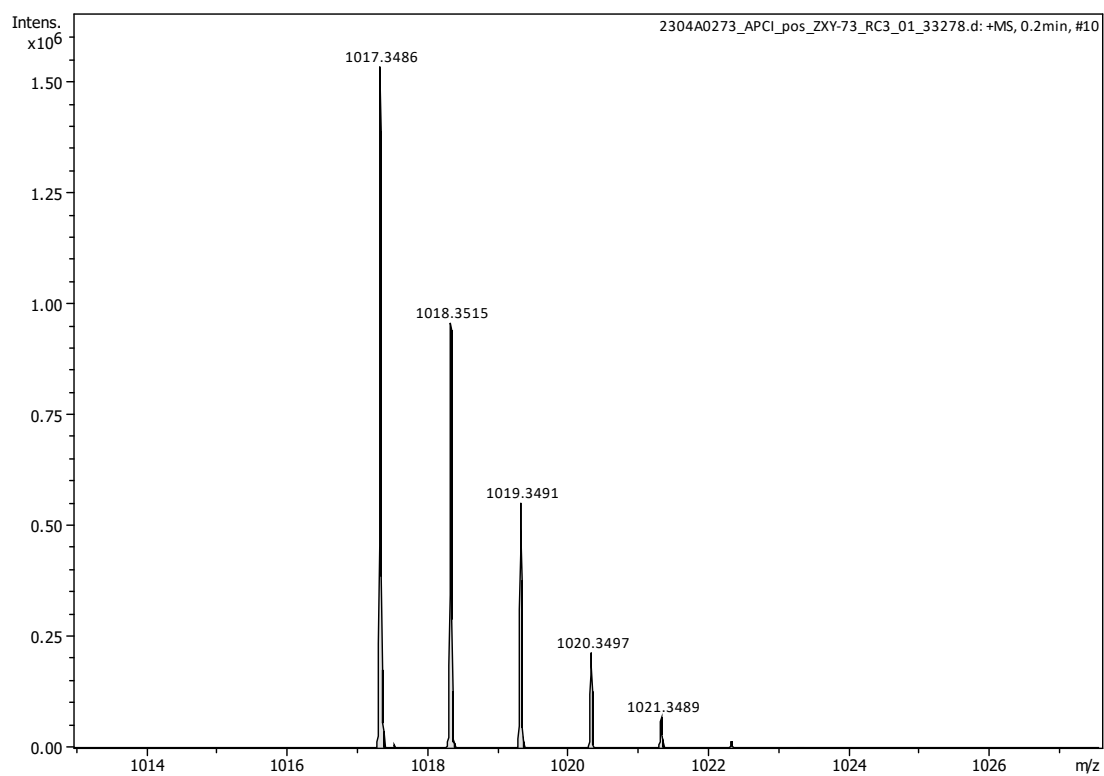


Figure S12. APCI-MS of gNR-Am.

### 3. TGA of Compounds

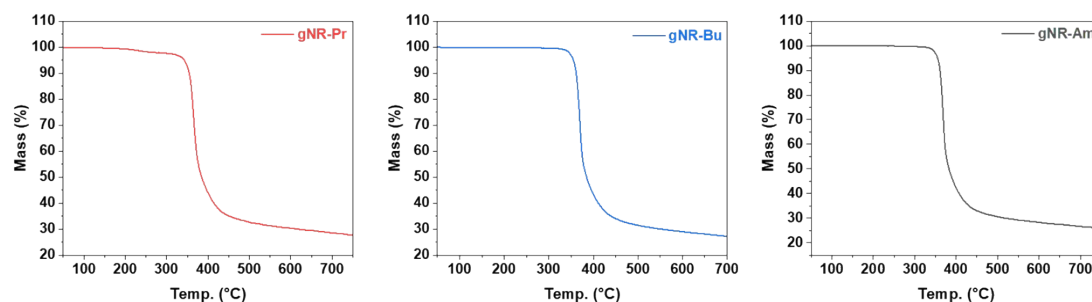


Figure S13. TGA of **gNR-Pr**, **gNR-Bu**, and **gNR-Am** measured in nitrogen.

### 4. CV of Compounds

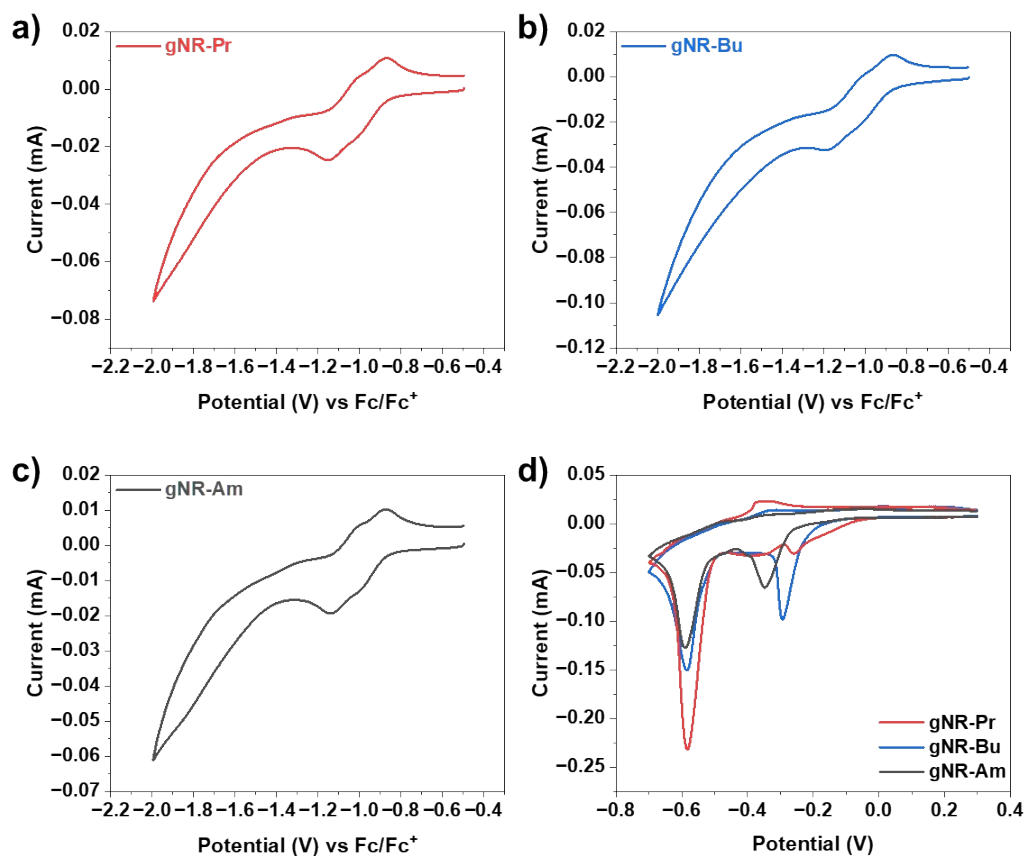


Figure S14. Cyclic voltammograms of a) **gNR-Pr**, b) **gNR-Bu**, and c) **gNR-Am** in chloroform solution with 0.1 M  $n\text{-Bu}_4\text{NPF}_6$  as supporting electrolyte at a scan rate of  $0.1 \text{ V s}^{-1}$ . The potential of Ag/AgCl reference electrode was internally calibrated against ferrocene; d) Cyclic voltammograms of **gNR-Pr**, **gNR-Bu**, and **gNR-Am** in a 0.1 M NaCl (aq) electrolyte at a scan rate of  $0.1 \text{ V s}^{-1}$ .

## 5. Detailed Data of GIWAXS Tests

**Table S1.** Solid states packing parameters of **gNR-Pr**, **gNR-Bu**, and **gNR-Am** in the out-of-plane direction (OOP).

		<b>gNR-Pr</b>	<b>gNR-Bu</b>	<b>gNR-Am</b>
<b>Lamellar packing (100)</b>	q ( $\text{\AA}^{-1}$ )	0.427	0.352	0.356
	d-spacing ( $\text{\AA}$ )	14.71	17.85	17.85
	FWHM( $\text{\AA}^{-1}$ )	0.0340	0.0336	0.0385
	CL( $\text{\AA}$ )	166.32	168.25	146.96
<b>Lamellar packing (200)</b>	q ( $\text{\AA}^{-1}$ )	0.864	0.716	0.719
	d-spacing ( $\text{\AA}$ )	7.27	8.78	8.74
<b>Lamellar packing (300)</b>	q ( $\text{\AA}^{-1}$ )		1.074	1.083
	d-spacing ( $\text{\AA}$ )	N/A	5.85	5.80
<b><math>\pi</math>-<math>\pi</math> packing (010)</b>	q ( $\text{\AA}^{-1}$ )	1.730	1.625	1.574
	d-spacing ( $\text{\AA}$ )	3.63	3.87	3.99
	FWHM( $\text{\AA}^{-1}$ )	0.1666	0.3149	0.5196
	CL ( $\text{\AA}$ )	33.94	17.96	10.88
	g (%)	12.4	17.6	22.9

**Table S2.** Solid states packing parameters of **gNR-Pr**, **gNR-Bu**, and **gNR-Am** in the in-plane direction (IP).

		<b>gNR-Pr</b>	<b>gNR-Bu</b>	<b>gNR-Am</b>
<b>Lamellar packing (100)</b>	q ( $\text{\AA}^{-1}$ )	0.391	0.494	0.492
	d-spacing ( $\text{\AA}$ )	16.07	12.72	12.77
	FWHM( $\text{\AA}^{-1}$ )	0.0423	0.0393	0.0447
	CL( $\text{\AA}$ )	133.56	143.85	126.51
<b>Lamellar packing (200)</b>	q ( $\text{\AA}^{-1}$ )	0.785		
	d-spacing ( $\text{\AA}$ )	8.00	N/A	N/A
<b><math>\pi</math>-<math>\pi</math> packing (010)</b>	q ( $\text{\AA}^{-1}$ )	1.668	1.823	1.785
	d-spacing ( $\text{\AA}$ )	3.77	3.45	3.52
	FWHM( $\text{\AA}^{-1}$ )	0.1065	0.0911	0.1286
	CL ( $\text{\AA}$ )	53.09	68.95	43.96
	g (%)	10.1	8.9	10.7
<b><math>\pi</math>-<math>\pi</math> packing (020)</b>	q ( $\text{\AA}^{-1}$ )	1.920		
	d-spacing ( $\text{\AA}$ )	3.27	N/A	N/A

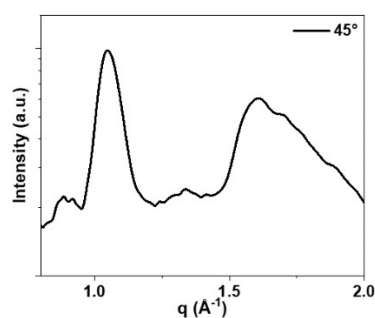


**Fig. S15** 1D GIWAXS chart extracted by integration along 45° direction.

## 6. AFM of compounds

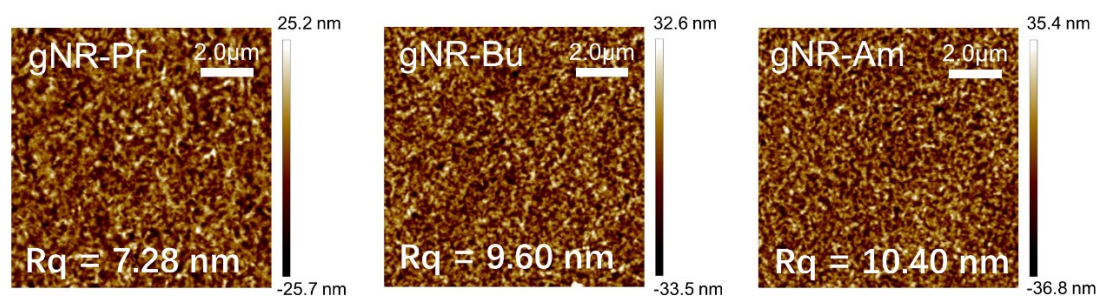


Figure S16. AFM height images of thin films coated from dissolved gNRs.

## 7. Organic Electrochemical Transistors Characterization

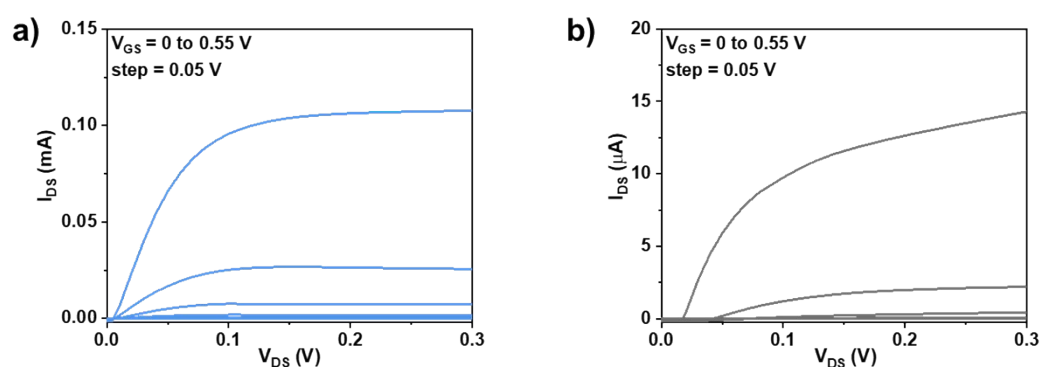


Figure S17. Output curves of OECT devices based on gNR-Bu and gNR-Am.

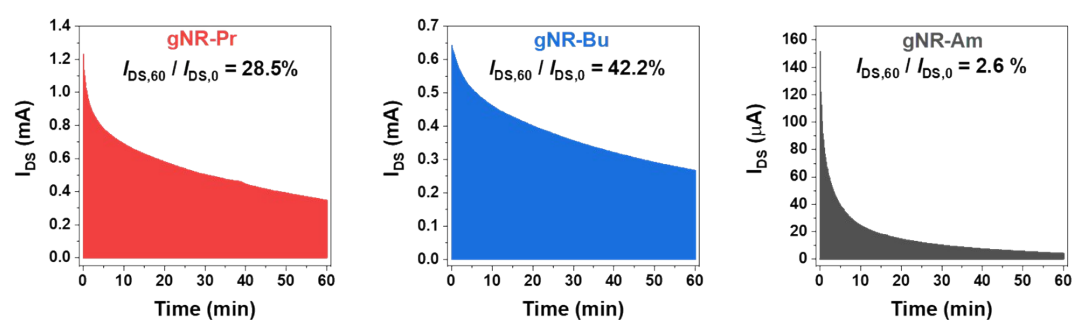
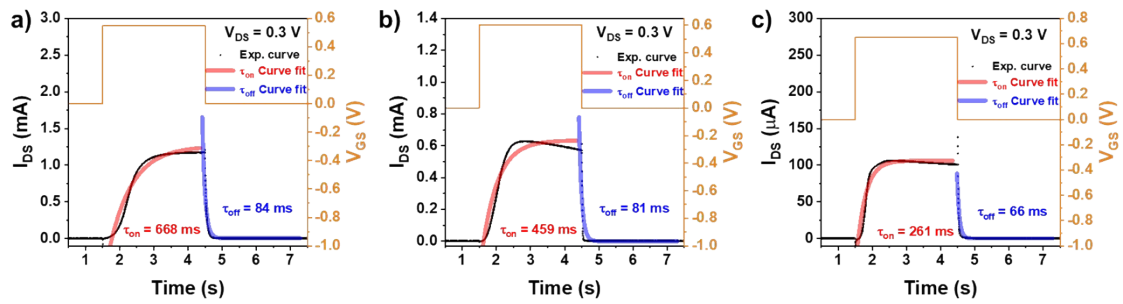
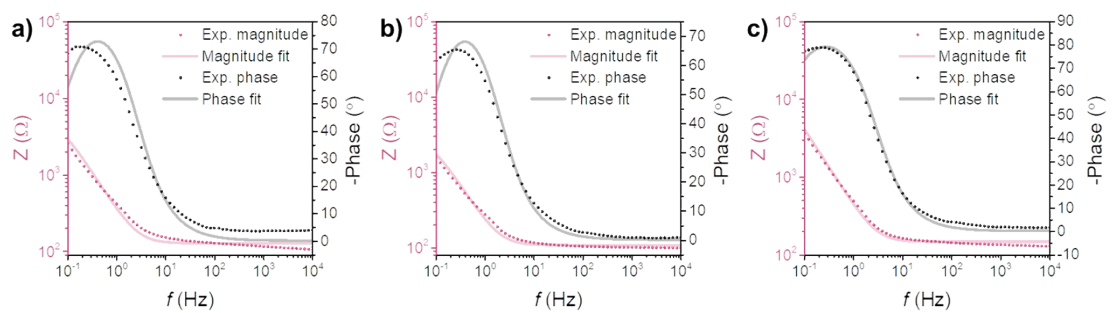


Figure S18. Operational stabilities of gNR-Pr, gNR-Bu, and gNR-Am over 1 hour's continuous electrochemical cycling with an alternating gate potential ranging from 0 V to 0.55 V and a pulse duration of 6 s for OECT channels biased at 0.3 V in 0.1M NaCl (aq) as ambient circumstance.



**Figure S19.** On & OFF time constant of a) **gNR-Pr**, b) **gNR-Bu**, and c) **gNR-Am** based OECT devices.



**Figure S20.** Electrochemical impedance spectroscopy of a) **gNR-Pr**, b) **gNR-Bu**, and c) **gNR-Am**. The curves were fitted *via*  $R_s (R_p // C)$  circuit model.

## 8. Organic Electrochemical Neuronal Synapse Characterization

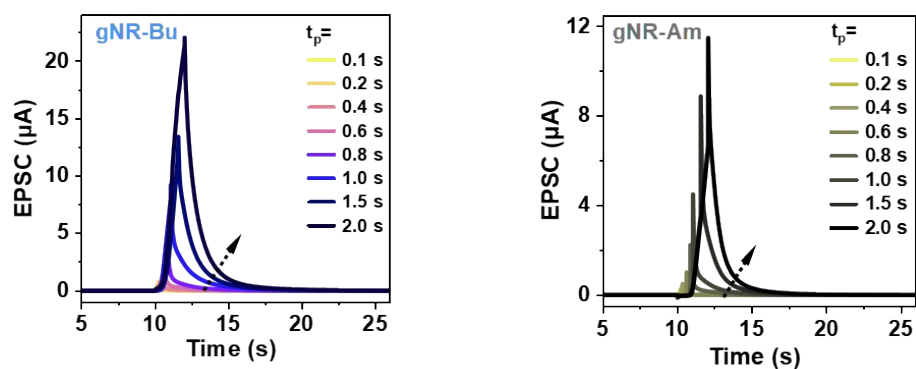


**Figure S21.** Single-pulse-induced spiking-timing-dependent plasticity of **gNR-Bu** and **gNR-Am** with different pulse duration ranging from 0.1 s to 2.0 s.

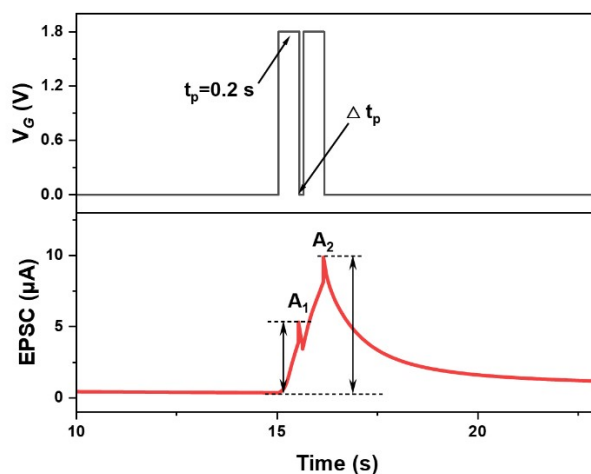


**Figure S22.** Paired-pulse facilitation diagram of **gNRs** based devices.

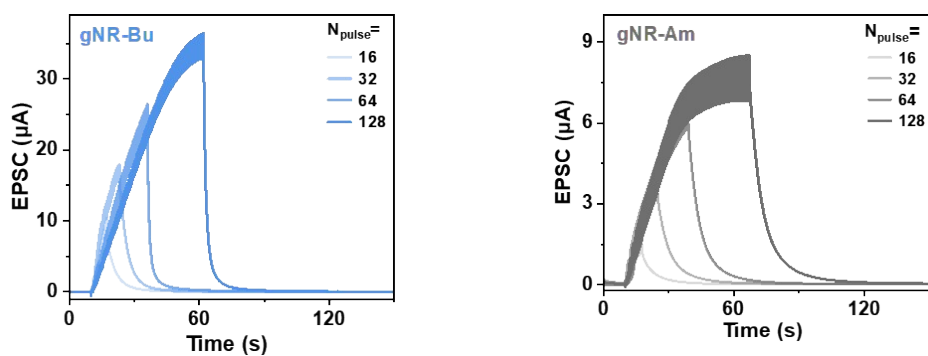


**Figure S23.** Long-term plasticity behavior of **gNR-Bu** and **gNR-Am** based devices.

## 9. References

- [1] F. Aryanasab, A. Shokri, M.R. Saidib, *Sci. Iran.*, 2013, **20**(6), 1833-1838.
- [2] R. Liu, X. Zhu, J. Duan, J. Chen, Z. Xie, C. Chen, X. Xie, Y. Zhang and W. Yue, *Angew. Chem. Int. Ed.*, 2024, **63**, e202315537.